Results in Materials 21 (2024) 100532

Contents lists available at ScienceDirect

Results in Materials

journal homepage: www.sciencedirect.com/journal/results-in-materials

Improving wear performance, physical, and mechanical properties of iron sand/epoxy composite modified with carbon powder

Nurul Fitria Apriliani [a,*], Willy Artha Wirawan [a,b,h,**], Mukhlis Muslimin [c], R.A. Ilyas [d,e,f,g], Muchamat Ardistya Rahma [a], Alfi Tranggono Agus Salim [h]

[a] Indonesian Railway Polytechnic, Tirta Raya Street, Nambangan Lor, Manguharjo, Madiun, 63161, Indonesia
[b] Department of Aircraft Engineering, Politeknik Penerbangan Surabaya, Jemur Andayani I No 73 Wonocolo, Surabaya, Indonesia
[c] Mechanical Engineering Department, Khairun University, Jl. Pertamina Kampus II Unkhair Gambesi, Ternate City, 97719, Indonesia
[d] Department of Chemical Engineering, Faculty of Chemical and Energy Engineering, Universiti Teknologi Malaysia, 81310, Johor Bahru, Johor, Malaysia
[e] Centre for Advanced Composite Materials, Universiti Teknologi Malaysia, Skudai, 81310, Johor, Malaysia
[f] Institute of Tropical Forest and Forest Products (INTROP), Universiti Putra Malaysia, Serdang, 43400 UPM, Selangor, Malaysia
[g] Centre of Excellence for Biomass Utilization, Universiti Malaysia Perlis, Arau, 02600, Perlis, Malaysia
[h] Madiun State Polytechnic, Jl. Ring Road Barat, Winongo, Manguharjo, Madiun, 63162, Indonesia

ARTICLE INFO

Keywords:
Composite
Iron sand
Carbon powder
Mechanical properties
Wear performance

ABSTRACT

This study was conducted to investigate the usage of iron sand as composite reinforcement. The addition of carbon powder with variations of 15 wt%, 20 wt%, and 30 wt% is expected to enhance the interfacial bond between iron sand and epoxy matrix to be better. Physical and mechanical properties of the composite were investigated using a wear resistance test Pin on Disc method, shore-D hardness, bending test, X-ray diffraction (XRD), Fourier Transform Infrared (FTIR) and Scanning Electron Microscope (SEM). The results showed an increase in wear resistance and mechanical properties of composite due to the addition of carbon powder. This was confirmed by the fact that the HCP composite with 30 wt% carbon powder showed a good increase in wear resistance but a reduction in flexural properties and hardness values. Meanwhile, the LCP composite with 20 wt% carbon powder was recommended in terms of good flexural properties. The increased mechanical properties of composite were supported by composite crystallinity index value recorded to be 59.45 % from the XRD test. SEM analysis showed better dispersion and interfacial bonding for carbon powder and iron sand in the composite matrix. These results are expected to contribute to the new development of composite brake pad.

1. Introduction

Composite materials are discovered to be attractive for several reasons including their lightweight, high strength, corrosion resistance, and ease of formation [1]. This has led to their wide application in various industries such as aviation, production of household appliances, construction, infrastructure, automotive, transportation, corrosive environments, electrical components, energy, marine, and sports equipment [2]. In the field of railways, composite have also been used in some components such as railway bearings [3,4], interior of high-speed trains [5], and brake pads [6]. Moreover, carbon-based composite has been widely used in construction materials, marine, household appliances, and aerospace engineering [7,8]. Composite have also been used for reinforcement due to their high tensile strength, high specific strength [9,10], good elasticity [11], and dimensional stability [12].

The need for wear-resistant and heat-resistant polymer composites is currently continuing to increase, especially in the automotive, aviation and electronics fields [13]. Polymer composites are currently being developed with natural fibers as fillers because they improve the mechanical properties of composites such as high specific modulus, low cost and lightweight [14]. Polymer composite development is also carried out using various techniques including the hand-lay method. This method has proven to be superior when compared to the resin transfer molding method [15].

Wear-resistant properties of carbon at high temperatures, lightweight, and stability in the environment [16,17] are also observed to

* Corresponding author. Indonesian Railway Polytechnic, Tirta Raya street, Nambangan Lor, Manguharjo, Madiun, 63161 Indonesia.
** Corresponding author. Department of Aircraft Engineering, Politeknik Penerbangan Surabaya, Jemur Andayani I No 73 Wonocolo, Surabaya, Indonesia.
E-mail addresses: nurul.fitria@ppi.ac.id (N.F. Apriliani), willy@pengajar.ppi.ac.id (W.A. Wirawan).

https://doi.org/10.1016/j.rinma.2024.100532
Received 13 September 2023; Received in revised form 18 December 2023; Accepted 7 January 2024
Available online 11 January 2024

have led to the application of carbon-reinforced composite in the field of transportation, specifically in aircraft braking systems [18], cars, and high-speed trains [19]. This shows that carbon powder can improve mechanical properties of composite. According to De Costa et al., the addition of carbon powder increased the tensile strength, hardness, impact strength, flexural strength, and density of composite [20]. Zeng et al., also reported that the incorporation of carbon powder in cement composite improved the compressive strength and made the microstructure denser [21].

Epoxy-based composite were also discovered to exhibit good mechanical properties for applications in the automotive, construction, and aerospace industries. This was due to the good physical properties of epoxy resin, specifically in damp places as well as its lower shrinkage compared to polyester [22]. However, epoxy resin also has several disadvantages, requires a long polymerization time, is susceptible to cracking and high price. The addition of carbon to epoxy-based composite was reported to have increased the interfacial bond between the fiber and the matrix, thereby improving mechanical properties of composite. In carbon-modified epoxy composite, the tensile strength increased by 21.9 % while wear rate decreased by 93.4 % [23].

Iron sand is quite abundant in different areas of Indonesia such as Java, Sumatra, Aceh, East Nusa Tenggara, and Papua. According to the Ministry of Energy and Mineral Resources of The Republic of Indonesia, iron sand reserves in the country were estimated at 2 billion tonnes in 2022 and this was almost 1.7 % of the reserve in the whole world. It is currently mostly used to produce building materials or in the cement industry as a filler. Several studies have been conducted to develop the potential of iron sand for wider applications such as in magnetic materials [24–27].

Iron sand was used as a filler in this study due to its high thermal resistance as well as the possibility of producing composite with high strength because of its ability to assist the matrix in resisting unwanted deformations [24]. It was also observed to have good wear resistance which was expected to complement the resistance of carbon to abrasion in order to produce materials with this properties [28]. Iron sand is a ceramic material that has high hardness. The addition of iron sand is expected to increase the hardness of the composite when compared to composites that do not have iron sand added.

Carbon materials such as carbon black or Carbon Nano Tube (CNT) were observed to have been combined with carbonyl iron, ferrite, magnetite, and others in recent years to produce composite materials to be applied in the defense sector due to their good properties [29,30]. Iron sand/epoxy composite was reported to have some advantages including high mechanical strength and corrosion resistance while the weakness was linked to the relatively high weight [31]. Composite could also be degraded at high temperatures, thereby reducing its mechanical properties.

Carbon powder was selected due to its high chemical stability and good processability [32]. The addition of carbon to iron sand/epoxy resin composite was based on the need to increase mechanical strength and reduce wear for subsequent application in the brake block material for railways. Moreover, the lightweight, thermal properties, and good frictional performance of carbon were expected to be useful in producing composite brake blocks that meet the required standards [33]. This was necessary because the brake block composite materials were required to have some characteristics such as high mechanical strength to withstand friction during braking as well as good abrasion and heat resistance without experiencing significant degradation. Therefore, mechanical properties of composite produced were investigated with a focus on the hardness and bending properties. The intention was to ensure the hardness increased as more content of carbon powder was added. Furthermore, the physical properties and structure were also analyzed to determine the effect of carbon on the surface morphology and homogeneity. The specific wear value, which was one of the important factors of the material applied in the braking system, was also evaluated.

2. Materials and methodology

2.1. Material

Epoxy matrix were supplied by PT. Justus Kimia Raya, Surabaya Indonesia. Iron sand powder was obtained from the South Coast of Pacitan district, Indonesia, and purified using the separation or extraction process. In the first stage, iron sand was washed with water until it was clean and dried on a hot plate at 40 °C for 2 h. The second stage was to separate the dry sand using a permanent magnet and wash it with distilled water to remove dirt. In the third stage, sand was dried and sieved with 80-size mesh (Fig. 1) (see Fig. 2).

While carbon powder made from coconut shell was obtained from PT Multi Chemical Indotrading, Tangerang Indonesia. The carbon powder material that has been formed is pulverized using a balmilling tool for 24 h, then sieved with a particle size of 100 mesh. After that, the carbon powder was immersed in phosphoric acid solution with a concentration of 8 % for 24 h. Then, the carbon was washed using distilled water until the filtrate was neutral and filtered. The activated carbon formed was then dried using an oven at 100 °C for 1 h.

2.2. Composite manufacturing process

Composite specimens were produced using the closed mold Vacuum assisted-resin infusion (VARI) method [34]. The process focused on weighing each iron sand (IS), carbon powder (CP), and epoxy matrix (EM) according to the composition in Table 1. Composite material was placed in a mold according to the standards of each test as shown in Fig. 3, dried for 24 h, and heated in an oven for 2 h at 40 °C. The equipment used to produce composite based on the VARI method is presented in Fig. 3. The method was applied because it was considered economical and has the ability to provide better control for harmful volatiles emitted by the resin when compared to the open mold [35,36]. The principle of impregnation in the VARI method focused on flowing the mixture of iron sand/epoxy and carbon powder into the mold using vacuum suction to minimize the voids in composite. The mold was covered by a tight bag which was later vacuumed to ensure there was a difference in the air pressure on the outside and inside, thereby causing the bag to press evenly on composite product.

2.3. X-ray diffraction (XRD) analysis

XRD was applied to identify the crystalline phase in the materials by evaluating the lattice structure parameters to determine the particle size and single crystals. The x-ray pattern was obtained using XRD Philips X'pert MPD, USA with C_u-k_α radiation of 30 kV at 17.5 mA, a *step size* of 0.075°, and *a step scan* of 2.5/s was used at approximately 10°–110°. The degree of crystallinity was determined as the CI *(crystallinity index)* using the following equation.

$$CI = 1 - \frac{I\,101}{I\,002} \cdot 100$$

$$\%Cr = \frac{I\,002}{I\,001 + I\,002} \cdot 100$$

where, CI is the *crystallinity index,* Cr indicates crystallinity, while I_{101} & I_{002} are the maximum crystalline intensity peaks and amorphous parts, respectively. I_{002} relates to the Miller index (002) which is in the range of $2\theta = 22–23°$ while I_{101} is linked to the Miller index (001) at approx. $2\theta = 18°$

2.4. Fourier Transform Infrared (FTIR) analysis

FTIR test was used to determine the changes in the composition of composite with carbon powder using Shimadzu, IRPrestige-2, Japan. This was achieved by mixing 5 g of composite powder with 95 % KBr and

Fig. 1. Separation process for iron sand used as composite reinforcement material.

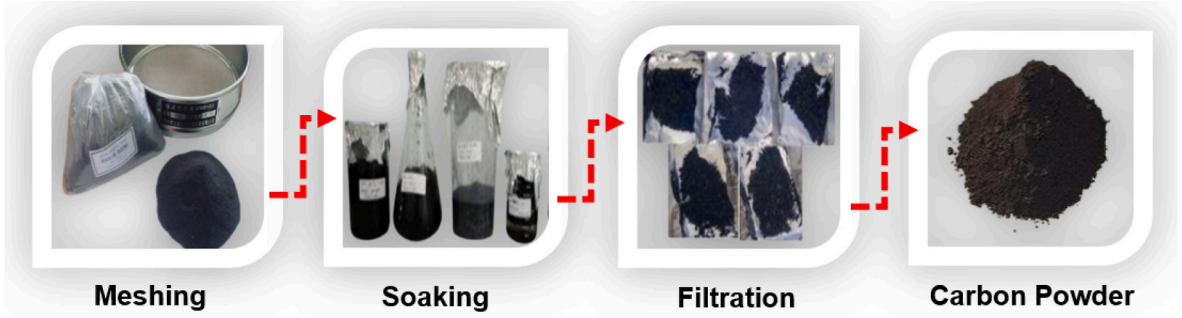

Fig. 2. Preparation process of carbon powder.

Table 1
Compositional variations in iron sand/epoxy composite modified with carbon powder.

Sample	Iron Sand	Carbon Powder	Epoxy Matrix
LCP (Low Carbon Powder)	15 %	15 %	70 %
MCP (Medium Carbon Powder)	15 %	20 %	65 %
HCP (High Carbon Powder)	15 %	30 %	55 %

inserting the mixture into the disk of the FTIR machine. The test was conducted by scanning each spectrum 32 times at a spatial resolution of 500–4000 cm^{-1} wavenumbers.

2.5. SEM analysis

Scanning Electron Microscopy (SEM) analysis was conducted to determine the morphology and topography of the specimen surface after fracture. The observations were made using HITACHI FlexSEM 1000, Japan to produce high resolution in high vacuum mode using an accelerated voltage of 20 kV Energy. It was conducted in the Environmental Laboratory of Institut Teknologi Sepuluh Nopember Surabaya and the samples were coated using Au–Pd before the test.

2.6. Wear test analysis

Composite wear analysis was conducted using the pin-on-disc method through the application of Oghosi High-Speed Universal Wear Testing, OAT-U Type, Japan. Moreover, the specimens used were produced at a dimension of 30 mm length, 20 mm width, and 10 mm height based on the ASTM G99 standard. The flat surface of the specimen was mounted on a holder (pin) and a pressure of 2.12 kg was applied on the rotating disc. The disc material used was made of DIN X 153 CrMoV 12 steel with a hardness of 54 RC. Furthermore, the friction test was conducted directly using the load cell on the machine based on the distance traveled. The process was applied to each specimen twice to collect test data and wear value was later calculated using the following equation.

$$Ws = \frac{B \times b^3}{8 \times r \times P_0 \times l_0} = \left(mm^2 / Kg\right)$$

where, Ws is the specific wear value (mm^2/kg), B is the width of wear plate (mm), b^3 is the width of wear on the specimen (mm), r is the radius of wear plate (mm), p_0 is the compressive force during wear process (kg), and l_0 is the distance traveled (mm).

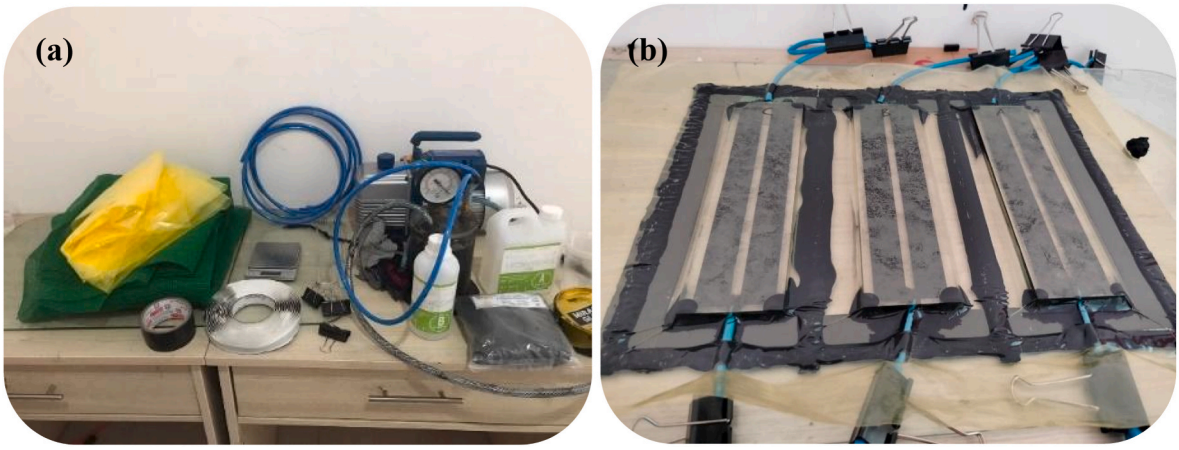

Fig. 3. VARI composite manufacturing method (a) tools and materials (b) specimen molding process composite.

2.7. Hardness test

The first step after composite had been printed was to prepare specimens at a dimension of 50 mm length, 50 mm width, and 5 mm thickness. The specimens were later placed in a room with a temperature of 23^{O}C and Relative Humidity (RH) of 50 % for a minimum of 40 h. This was followed by the Shore-D penetration test using GS-720 N Teclock Durometer, Japan with a load of 5 kg (49 N). Data were recorded at a range of 1 s and 15 s, the test was repeated five times, and the average value was determined.

2.8. Flexural strength test

A bending test was conducted to determine the flexural strength value of composite based on ASTM D790 standard procedures. This was achieved using a specimen that was 152 mm long, 25.4 mm wide, and 6 mm thick. A Universal Testing Machine, TARNO GROCKI, UPH-100 kN, was used using three-point bending with a speed of 2 mm/s and a distance of 60 mm between the supports [37]. The bending strength was calculated using the following equation.

$$b = \frac{3.P.L}{2.\ B.H^2}$$

where, σb is the flexural strength value from the bending test, P is the load (N), L is the length of the span between the fulcrums (mm), B is the width of the specimen (mm), and H is the thickness (mm)

3. Results and discussion

3.1. XRD analysis

The diffractogram of carbon-reinforced iron sand/epoxy composite material is shown in Fig. 4. The amorphous peak in the LCP specimen was found at an angle of 2θ = 20°-60^{0} with an intensity of 762 while the MCP had 2θ = 21.08^{0} with 663 and HCP had 2θ = 22.34^{0} with 366 respectively. This showed that the HCP produced the lowest intensity because composite was not filled with carbon evenly, thereby leading to the absence of a perfect bond between carbon and the epoxy resin. The peak was associated with the basic constituent material, carbon powder, which was reported to have the highest peak at approximately 2θ = 20°-30^{0} [38,39] (see Fig. 5).

The observation was further supported by the results of the SEM test explained in the next section. It was discovered that the peaks produced by all the specimens did not have sharp edges and the broadness indicated the amorphous nature of carbon composite [40,41]. The results showed that HCP produced wider peaks and lower crystallinity than the other specimens and this meant it was more amorphous than the LCP and MCP. The XRD peak was observed to generally shift to the right as the content of carbon in the mixture increased and this was associated with the addition of amorphous carbon which led to the overlapping of the previous diffraction peaks.

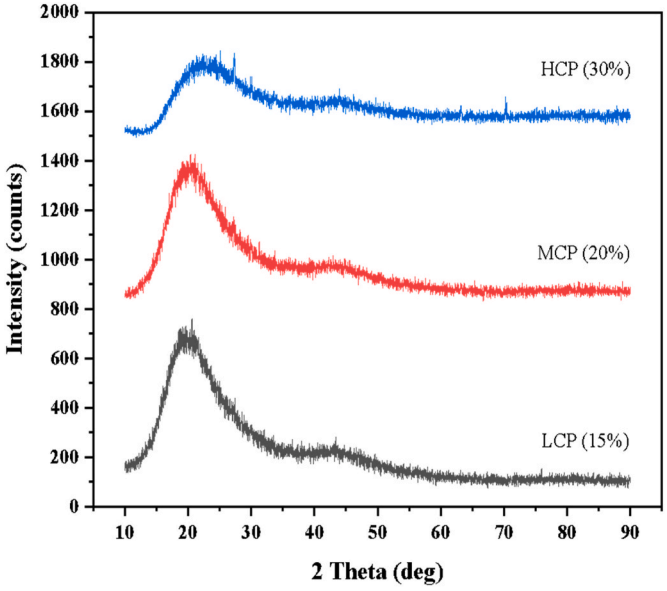

Fig. 4. The diffractogram of iron sand/epoxy composite modified with carbon powder.

The crystallinity index of the LCP, MCP, and HCP composite is presented in Fig. 4. The results showed that carbon powder content in composite influenced the structure, crystallinity, and properties of composite [42]. The increase in diffraction intensity of each specimen indicated the increasing number of crystals contained in composite. The crystallinity index value for the LCP composite was 46.92 % while MCP had 59.45 % and the HCP had 45.08 %. The high values recorded were observed to have confirmed the better mechanical properties reported for each composite. The increase in the crystallinity index was discovered to be due to the increment in the crystal size and the loss of amorphous properties in composite. MCP with 20 wt% carbon powder had a higher value compared to the HCP with 30 wt% and this was possibly due to the high content of carbon added which made the material to be amorphous. It could also be because the atoms were disordered and did not have a clear crystal pattern, thereby making the material lose its crystalline characteristics. Therefore, it is important to

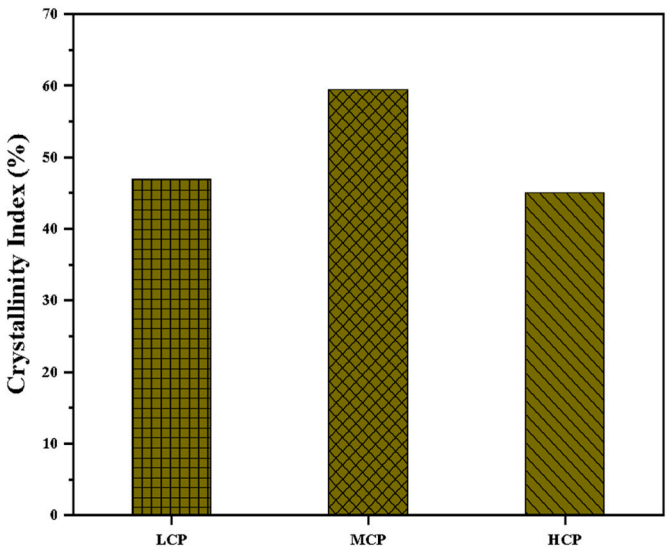

Fig. 5. X-ray crystallinity Index of iron sand/epoxy composite modified with carbon powder.

consider the concentration of additional ingredients such as carbon in the process of developing composite to ensure the crystalline structure is maintained and the desired mechanical properties can be achieved. MCP composite with 20 wt% carbon powder was recommended to produce composite for several applications.

3.2. FTIR analysis

The three spectra of composite formed by adding different wt.% of carbon are presented in Fig. 6 and they were all observed to have a similar peak pattern. The FTIR results showed that the only difference observed was in the absorption intensity. Moreover, the peaks identified at 653 cm^{-1} indicated C–H bending while those at 775 cm^{-1} were aromatic C═C. The stretching frequencies of the C–O produced peak at 1051 -1301 cm^{-1} indicating the C–O bond stretching of the epoxy and alkoxy groups and explaining the presence of epoxy groups in composite [43,44]. Meanwhile, 1124 cm^{-1} was classified as C–O stretching vibration from epoxy [45], 2310 cm^{-1} was C═O stretching, the region

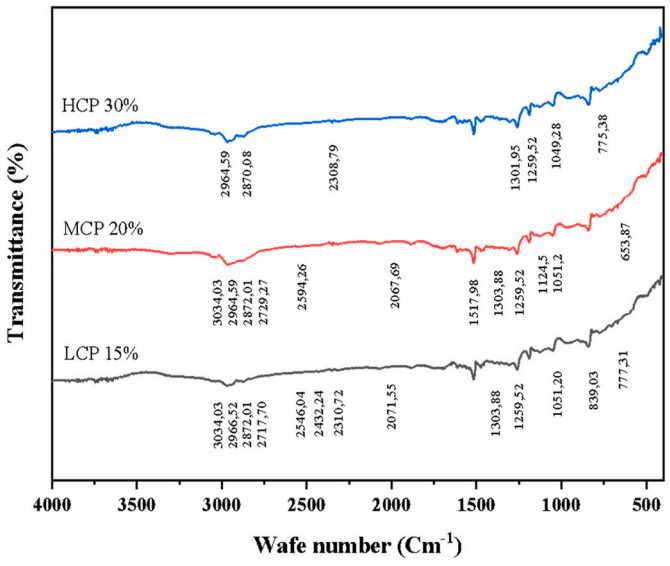

Fig. 6. FTIR spectra of iron sand/epoxy composite modified with carbon powder.

around 1517 cm^{-1} was aromatic C═C bonds with graphite as the principal bond [38], those close to 2717 cm^{-1} were aldehyde group, and 2964 cm^{-1} were due to aromatic C–H groups. These were found to be the characteristic peaks of epoxy resin in forming composite structure with carbon powder [46].

3.3. SEM analysis

The morphology of each composite with carbon powder is presented in Fig. 7. The SEM observations showed that carbon powder was dispersed effectively and relatively uniform in the LCP composite. However, the surface had a slight crack which had the ability to reduce the flexural strength. The cracking could be due to the higher percentage of matrix compared to reinforcement. The matrix generally had weaker properties and could be damaged under a load by cracking, delaminating, or peeling from the reinforcing material.

The MCP composite was observed to have a dense and uniform structure with carbon powder distributed effectively in the epoxy matrix to provide significant structural reinforcement. The surface showed a good bond between iron sand, carbon powder, and epoxy matrix, and the SEM images indicated there was no slightest crack. The results proved that composite was able to bond well and this contributed to the bending resistance.

The distribution of carbon powder in the epoxy matrix of HCP was not homogeneous. Carbon powder tended to form agglomerations or clumps and this led to a non-uniform structure in composite. This made the bond between carbon powder and the epoxy matrix weaker, leading to a significant reduction in the resistance of composite to bending strength. The addition of a high volume of carbon powder could trigger the initial failure of composite due to the hard nature of carbon and the presence of large pores. SEM observations also showed that HCP composite tended to be brittle and cracked or broke easily. However, the addition of wt% carbon powder improved the hardness and wear resistance of HCP composite despite these weaknesses.

3.4. Composite wear analysis

The addition of carbon powder to iron sand composite and epoxy matrix was observed to have affected wear rate as presented in the results presented in Table 3. This was indicated by the reduction in the specific wear of composite when carbon powder volume was added. The LCP composite was discovered to have a specific wear value of 1.81 × 10^{-6} mm^2/kg, MCP had 1.58 × 10^{-6} mm^2/kg, and HCP had 8.63 × 10^{-7} mm^2/kg. The reduction in wear rate could be associated with mechanical properties of carbon powder such as its high levels of wear and hardness. The particles in carbon powder acted as a filler to fill in the gaps between the epoxy matrix and iron sand in order to produce a solid composite with a high hardness value as shown in Table 2. Meanwhile, this hardness value was closely related to the specific wear as indicated by the fact that composite with harder resistance to friction had better wear. This was associated with the results of a previous study that good wear-resistance properties of composite could be influenced by the hard and abrasion-resistant properties of carbon powder [47]. The result also agreed with the findings of [48] that the coefficient of friction (CoF) for the glass-epoxy composite was reduced due to the addition of carbon. Moreover, the presence of carbon was also reported to have decreased the CoF in composite to 31 % due to its function as a solid lubricating material [49]. The CoF and wear levels were further discovered to be low in composite with a combination of carbon and epoxy [50]. This was linked to the ability of carbon structure to improve the tribological properties of composite based on its self-lubricating attribute (see Table 4).

3.5. Hardness value and flexural properties

Fig. 8 shows the hardness value for all the specimens with different

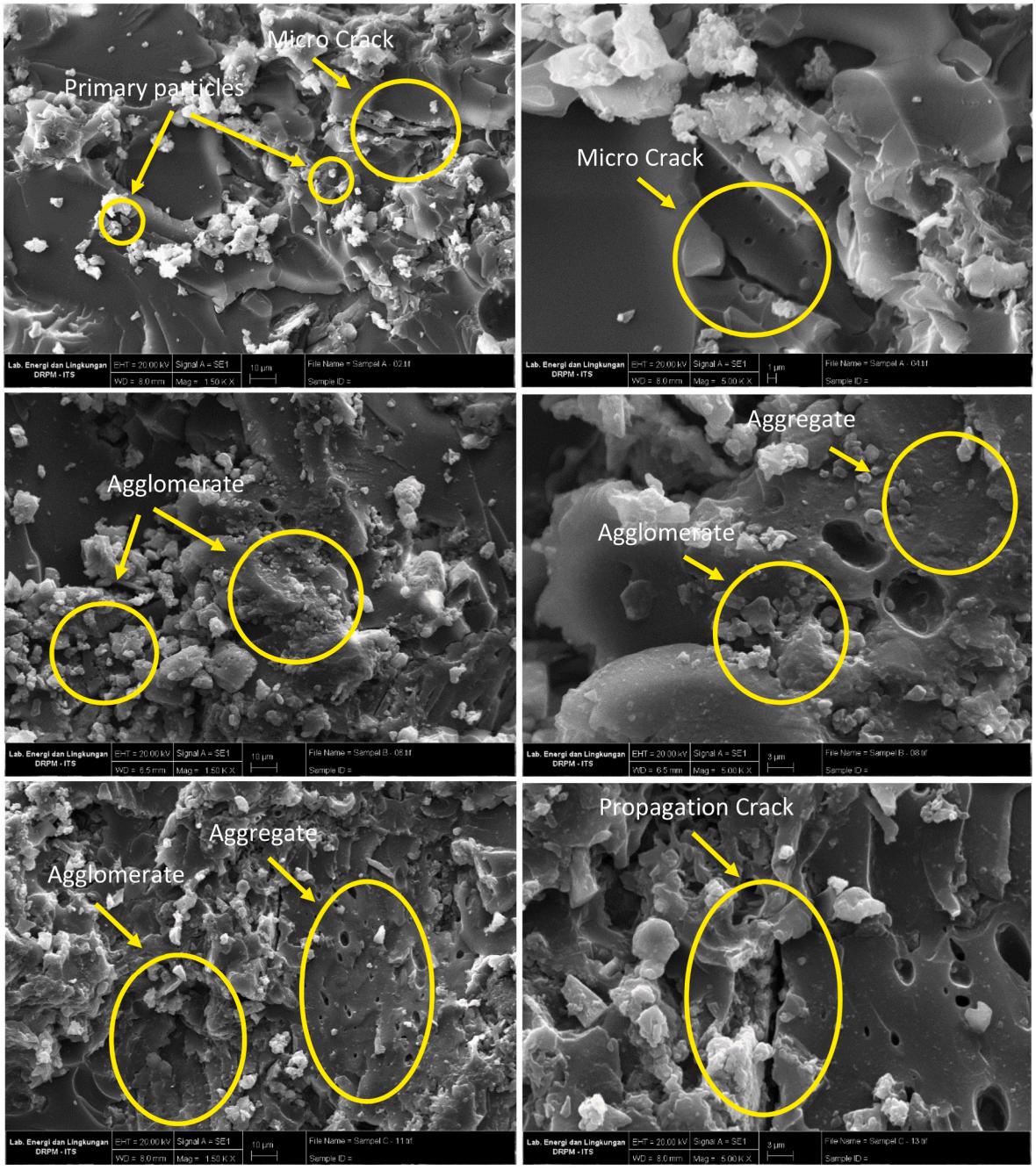

Fig. 7. SEM micrographs of iron sand/epoxy composite modified with carbon powder.

volumes of carbon and the trend indicated an increase in the hardness value as the content of carbon added to composite increased. This was observed from the 75.43 HD recorded for the LCP composite, 77.33 HD for the MCP, and 81.33 HD for the HCP. The information presented in Table 2 also confirmed this trend after the conversion of the value to HRR. Meanwhile, this hardness was believed to have been formed due to several factors including the usage of the epoxy resin, iron sand, and carbon powder as the materials for composite. The high hardness value of carbon was reported to have provided the dominant impact on the hardness recorded for composite [51]. The addition of a high amount of carbon increased the density of its particles in composite and this further enhanced the hardness [40,52]. Moreover, carbon powder was assumed to have filled the gap between the fiber and the matrix to produce a denser composite. This was linked to the reduction in the voids by filling the hollow nature of carbon with an epoxy matrix [53,54]. The increase in the hardness was also attributed to the homogeneous distribution of the mixture of carbon powder, iron sand, and epoxy resin as proven in the SEM test observations. This homogeneity improved the surface bond between the matrix and the reinforcement, thereby increasing the hardness of composite. The addition of foam from carbon powder significantly increased the Brinell hardness value of composite when compared to those produced from pure epoxy [55]. Urszula Szeluga et., al. (2020) also reported that the hardness increased by up to three folds and a similar trend was reported by Bal (2009) where carbon addition improved the hardness of the epoxy matrix up to 62 % with 0.75 % weight [56,57].

The flexural strength and modulus values for composite are presented in Fig. 9. The average for flexural strength for LCP was recorded to be 116.29 Mpa, MCP was 238.51 Mpa, and HCP was 126.33 Mpa while the flexural modulus was found to be 2531.4 Mpa, 2560.81 Mpa,

Table 2
Vibrational modes of functional groups in iron sand/epoxy composite modified with carbon powder.

Wavenumber (cm^{-1})			Functional group
LCP	MCP	HCP	
	653.87		C–H Bend
777,31		775.38	Aromatic C–H
839,03			C═C
1051,2	1051.2	1049.28	C–O Stretch
	1124.5		C–O Stretch
1259,52	1259.52	1259.52	C–O Stretch
1303,88	1303.88	1301.95	C–O Stretch
	1517.98		Aromatic C═C
2071,55	2067.69		N═C═S
2310,72		2308.79	C═O Stretch
2546,04	2594.26		S–H
2717,7	2729.27		Aromatic C–H
2872,01	2872.01	2870.08	Aromatic C–H
2966,52	2964.59	2964.59	Aromatic C–H
3034,03	3034.03		C–H Stretch
	3057.17		C–H Stretch

Table 3
Composite-specific wear of iron sand/epoxy composite modified with carbon powder.

specimen	b^3 (mm)	B (mm)	r (mm)	P_0 (kg)	l_0 (m)	*Specific Wear* (Ws) (mm^2/kg)
LCP	2.03 ± 0,314	3	13.06	2.12	66	1.81×10^{-6}
MCP	1.68 ± 0,900	3	13.06	2.12	66	1.58×10^{-6}
HCP	1.61 ± 0,076	3	13.06	2.12	66	$8.63\ 10^{-7}$

Table 4
Hardness value.

Specimen	Hardness (HD)	Hardness (HRR)
LCP	75,43 ± 0,196	90,88 ± 0,386
MCP	77,33 ± 0,884	94,66 ± 1766
HCP	81,33 ± 1761	102,66 ± 3524

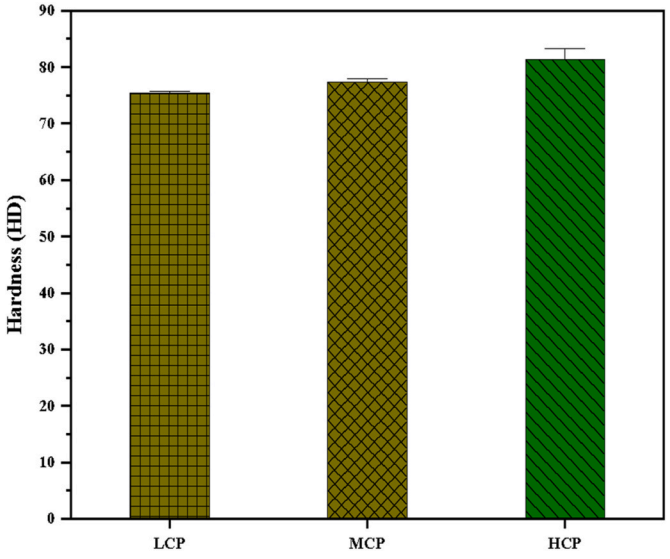

Fig. 8. The hardness value of iron sand/epoxy composite modified with carbon powder.

and 1018.05 Mpa respectively. This showed that the highest values for both were in the MCP composite with 20 wt% carbon powder and a similar trend was reported for the study on the Polyester-CHF composite where the addition of 10 % coconut shell powder had a higher flexural strength value compared to 5 % [58].

Meanwhile, HCP with 30 wt% carbon powder was observed to have the lowest was due to the non-uniform size and shape of carbon powder which led to unstable stresses and subsequently lower flexural strength and modulus. It is possible that there are fairly even voids. These voids result in fewer cohesive bonds between materials in the composite, thereby reducing the material's strength in facing pressure and resulting in a significant decrease in flexural strength. The carbon content is more dominant so that the epoxy resin is not too strong in binding carbon, thereby weakening the mechanical properties of the composite. Apart from that, during the mixing process, uneven mixing may occur. Another possible reason was the poor compatibility between the fiber and the matrix because of the high content of carbon powder used. This was linked to the hydrophilic properties of carbon powder as well as the hydrophobic attribute of epoxy [1]. The addition of 30 wt% carbon powder increased the hydrophilic properties of the mixture and limited the ability of the resin to bind perfectly. These results were confirmed in the photos obtained through SEM. Previous studies have also shown that the flexural strength and modulus produced by carbon/epoxy resin composite were better than pure epoxy resin [59]. This was associated with the reaction between carbon hybrid functional groups and the epoxy resin that strengthened the interfacial bond between these compounds [60]. The bond subsequently transmitted the stress from the matrix to the filler, thereby improving the flexural properties of the epoxy composite [61]. Another study by Chandramohan (2020) also showed an increase in the flexural strength of epoxy composite produced using the Vacuum Assisted Resin Infusion Molding (VARIM) method by 12 % due to the addition of 0.3 wt% carbon [62].

4. Conclusion

In conclusion, the factors that could be used to improve wear performance and mechanical properties of iron sand/epoxy composite modified with carbon powder have been discovered. The hardness value of the HCP composite with 30 wt% carbon powder increased by 81.33 HD or 102.66 HRR with significant specific wear of HCP 8.63×10^{-7} mm^2/kg but its flexural properties decreased. The results also showed that the LCP composite with 20 wt% carbon powder was recommended due to its high flexural strength of 238.51 MPa and modulus of 2560.81 MPa. The increase in mechanical properties was supported by the crystallinity index value of 59.45 % in the XRD test and the absence of a highly significant difference in the absorption intensity from the FTIR analysis. The results showed that the epoxy resin formed composite structure with carbon powder. This was further confirmed through the microstructural observations using SEM where carbon powder was observed to have better dispersion and interfacial bonding in composite matrix. Further studies are recommended to serve as a contribution to the development of industrial materials with high wear resistance performance and mechanical properties.

Funding

This study did not receive any specific grant from funding agencies in the public, commercial, or not-for-profit sectors.

CRediT authorship contribution statement

Nurul Fitria Apriliani: Formal analysis, Funding acquisition, Resources, Writing - original draft, Writing - review & editing. **Willy Artha Wirawan:** Conceptualization, Formal analysis, Resources, Writing - original draft, Writing - review & editing. **Mukhlis Muslimin:** Methodology, Software. **R.A. Ilyas:** Supervision, Validation. **Muchamat**

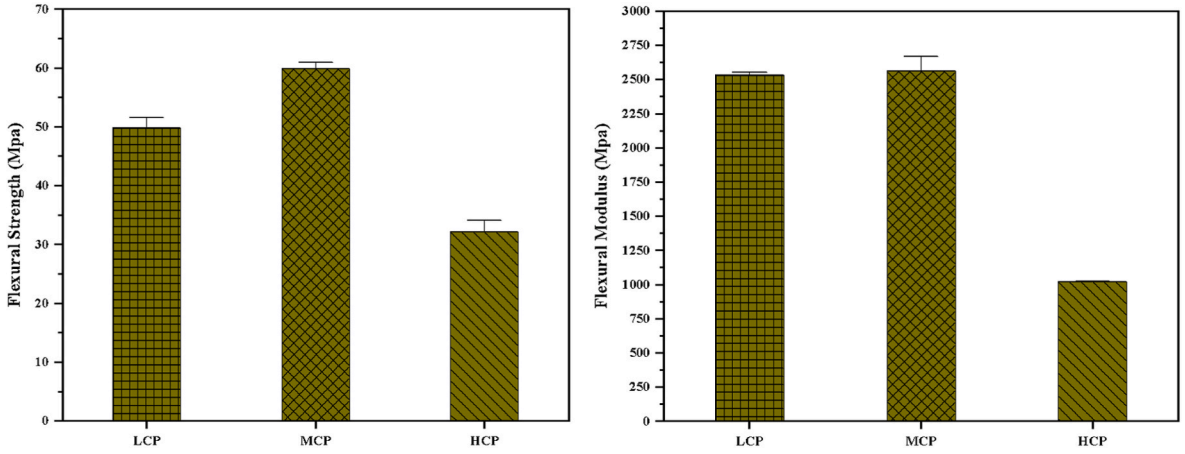

Fig. 9. (a) Flexural strength and (b) Flexural modulus of iron sand/epoxy composite modified with carbon powder.

Ardistya Rahma: Data curation, Funding acquisition, Investigation, Project administration. **Alfi Tranggono Agus Salim:** Data curation, Project administration, Resources.

Declaration of competing interest

The authors declare that they have no known competing financial interests or personal relationships that could have appeared to influence the work reported in this paper.

Data availability

Data will be made available on request.

References

[1] W.A. Wirawan, A. Sabitah, M.A. Choiron, M. Muslimin, A. Zulkarnain, B. W. Budiarto, Effect of chemical treatment on the physical and thermal stabillity of Hibiscus Tiliaceus Bark Fiber (HBF) as reinforcement in composite, Results Eng 18 (April) (2023) 101101, https://doi.org/10.1016/j.rineng.2023.101101.

[2] M. Muslimin, et al., 'The effect of liquid smoke treatment on physical stability and impact toughness chicken, CFF 52 (6) (2023) 1845–1854.

[3] X. Wang, L. Lei, H. Yu, A Review on Microstructural Features and Mechanical Properties of Wheels/Rails Cladded by Laser Cladding, 2021.

[4] Z. Zeng, A. Ahmed Shuaibu, F. Liu, M. Ye, W. Wang, Experimental study on the vibration reduction characteristics of the ballasted track with rubber composite sleepers, Construct. Build. Mater. 262 (2020) 120766, https://doi.org/10.1016/j.conbuildmat.2020.120766.

[5] J. Zhang, D. Yao, R. Wang, X. Xiao, Vibro-acoustic modelling of high-speed train composite floor and contribution analysis of its constituent materials, Compos. Struct. 256 (2021) 113049, https://doi.org/10.1016/j.compstruct.2020.113049. May 2020.

[6] Y. Xiao, et al., Mechanical and tribological behaviors of copper metal matrix composites for brake pads used in high-speed trains, Tribol. Int. 119 (2018) 585–592, https://doi.org/10.1016/j.triboint.2017.11.038. July 2017.

[7] M.B. Hunain, S.N. Alnomani, Q. Razzaq, An investigation of tensile and thermal properties of epoxy polymer modified by activated carbon particle, IOP Conf. Ser. Mater. Sci. Eng. 1094 (1) (2021) 012164, https://doi.org/10.1088/1757-899x/1094/1/012164.

[8] J. Yao, H. Chang, T. Zhang, Y. Niu, Synergistic toughening in the interleaved carbon fibre reinforced epoxy composites by thermoplastic resin and nanomaterials, Polym. Test. 115 (August) (2022) 107769, https://doi.org/10.1016/j.polymertesting.2022.107769.

[9] W.A. Wirawan, M.A. Choiron, E. Siswanto, T.D. Widodo, Analysis of the fracture area of tensile test for natural woven fiber composites (hibiscus tiliaceus-polyester), J. Phys. Conf. Ser. 1700 (1) (2020), https://doi.org/10.1088/1742-6596/1700/1/012034.

[10] T. Deng, et al., Structure and properties of Bombyx mandarina silk fiber and hybrid silk fiber, J. Nat. Fibers (2019) 1–13, https://doi.org/10.1080/15440478.2019.1623743. Jun.

[11] A. Wang, X. Liu, Q. Yue, G. Xian, Hydrothermal durability of unidirectional flax/carbon fiber hybrid composite plates, J. Mater. Res. Technol. 22 (2023) 2043–2061, https://doi.org/10.1016/j.jmrt.2022.12.021.

[12] Y. Singh, J. Singh, S. Sharma, T.-D. Lam, D.-N. Nguyen, Fabrication and characterization of coir/carbon-fiber reinforced epoxy based hybrid composite for helmet shells and sports-good applications: influence of fiber surface modifications on the mechanical, thermal and morphological properties, J. Mater. Res. Technol. 9 (6) (2020) 15593–15603, https://doi.org/10.1016/j.jmrt.2020.11.023.

[13] V. Tambrallimath, R. Keshavamurthy, P.G. Koppad, D. Sethuram, Mechanical characterization of PC-abs reinforced with CNT nanocomposites developed by Fused deposition modelling, J. Phys. Conf. Ser. 1455 (2020), https://doi.org/10.1088/1742-6596/1455/1/012003.

[14] A. Gunge, P.G. Koppad, M. Nagamadhu, S.B. Kivade, K.V.S. Murthy, Study on mechanical properties of alkali treated plain woven banana fabric reinforced biodegradable composites, Compos. Commun. 13 (2019) 47–51, https://doi.org/10.1016/j.coco.2019.02.006. December 2018.

[15] K.C. Nagaraja, S. Rajanna, G.S. Prakash, P.G. Koppad, M. Alipour, Studying the effect of different carbon and glass fabric stacking sequence on mechanical properties of epoxy hybrid composite laminates, Compos. Commun. 21 (2020) 100425, https://doi.org/10.1016/j.coco.2020.100425. July.

[16] S. Fan, L. Zhang, L. Cheng, J. Zhang, S. Yang, H. Liu, Wear mechanisms of the C/SiC brake materials, Tribol. Int. 44 (1) (2011) 25–28, https://doi.org/10.1016/j.triboint.2010.09.003.

[17] X. Ma, et al., Flexural strength and wear resistance of C/C–SiC brake materials improved by introducing SiC ceramics into carbon fiber bundles, Ceram. Int. 47 (17) (2021) 24130–24138, https://doi.org/10.1016/j.ceramint.2021.05.124.

[18] R. Gadow, M. Jiménez, Carbon fiber-reinforced carbon composites for aircraft brakes, Am. Ceram. Soc. Bull. 98 (6) (2019) 28–34.

[19] V.V. Alisin, Tribological tests of frictional carbon/carbon composite in braking mode, IOP Conf. Ser. Mater. Sci. Eng. 941 (1) (2020), https://doi.org/10.1088/1757-899X/941/1/012066.

[20] T.C. Dias, T.H. Panzera, R.T.S. Freire, C.T. Garcia, J.C. Santos, 'Epoxy Polymers Reinforced with Carbon Powder Wastes', No. January, 2018, pp. 826–832, https://doi.org/10.21452/bccm4.2018.14.04.

[21] L. Wang, F. Aslani, Piezoresistivity performance of cementitious composites containing activated carbon powder, nano zinc oxide and carbon fibre, Construct. Build. Mater. 278 (2021) 122375, https://doi.org/10.1016/j.conbuildmat.2021.122375.

[22] H. Abdellaoui, M. Raji, R. Bouhfid, A. el kacem Qaiss, Investigation of the deformation behavior of epoxy-based composite materials, Fail. Anal. Biocompos. Fibre Rein Compos. Hybrid Compos. (2018) 29–49, https://doi.org/10.1016/B978-0-08-102293-1.00002-4.

[23] H. Nie, et al., Optimizing mechanical and biotribological properties of carbon fiber/epoxy composites by applying interconnected graphene interface, Appl. Surf. Sci. 604 (2022) 154432, https://doi.org/10.1016/J.APSUSC.2022.154432. Dec.

[24] A. Taufiq, et al., Synthesis of magnetite/silica nanocomposites from natural sand to create a drug delivery vehicle, Heliyon 6 (4) (2020), https://doi.org/10.1016/j.heliyon.2020.e03784.

[25] A.M.S. Sebayang, et al., Nano-structures and magnetic properties of Zn1-xCux/2Nix/2Fe2O4 (x = 0-0.4) synthesized from natural iron sand, South Afr. J. Chem. Eng. 42 (July) (2022) 216–222, https://doi.org/10.1016/j.sajce.2022.08.013.

[26] B. Satria, Z. Masrurah, S.J. Fajar, Magnetic susceptibility and grain size distribution as prospective tools for selective exploration and provenance study of iron sand deposits: a case study from Aceh, Indonesia, Heliyon 7 (12) (2021) e08584, https://doi.org/10.1016/j.heliyon.2021.e08584.

[27] T. Sembiring, D. Siburian, M. Rianna, ZnMnFe2O4 particle synthesized by natural iron sand for making permanent magnetic material, Mater. Sci. Energy Technol. 6 (2023) 124–129, https://doi.org/10.1016/j.mset.2022.12.005.

[28] M. Rianna, et al., Effect of calcination temperature on Microstructures, magnetic properties, and microwave absorption on BaFe 11.6 Mg 0.2 Al 0.2 O 19 synthesized from natural iron sand, Case Stud. Therm. Eng. 13 (2019), https://doi.org/10.1016/j.csite.2019.100393. November 2018.

[29] S. Mishra, V. Pratap, A.K. Chaurasia, A.K. Soni, A. Dubey, A.K. Dixit, Combined effect of exfoliated graphite/ferrite filled epoxy composites on microwave absorbing and mechanical properties, Phys. Open 14 (2023), https://doi.org/10.1016/j.physo.2023.100138. December 2022.

[30] Q. Xia, Z. Zhang, Y. Liu, J. Leng, Buckypaper and its composites for aeronautic applications, Compos. Part B Eng. 199 (2020) 108231, https://doi.org/10.1016/j.compositesb.2020.108231. February.
[31] Z. Shahryari, K. Gheisari, M. Yeganeh, B. Ramezanzadeh, Designing a dual barrier-self-healable functional epoxy nano-composite using 2D-carbon based nano-flakes functionalized with active corrosion inhibitors, J. Mater. Res. Technol. 22 (2023) 2746–2767, https://doi.org/10.1016/j.jmrt.2022.12.138.
[32] Y. Li, D. Li, H. Cheng, C. Han, L. Xiao, Morphology and physical properties of composites based on high-density polyethylene/propylene-ethylene random copolymers blends and carbon black, Polym. Test. 123 (February) (2023), https://doi.org/10.1016/j.polymertesting.2023.108050.
[33] S. Wu, Y. Liu, Y. Ge, L. Ran, K. Peng, M. Yi, Structural transformation of carbon/carbon composites for aircraft brake pairs in the braking process, Tribol. Int. 102 (2016) 497–506, https://doi.org/10.1016/j.triboint.2016.06.018.
[34] W.A. Wirawan, Surface modification with silane coupling agent on tensile properties of natural fiber composite, J. Energy, Mech. Mater. Manuf. Eng. 2 (2) (2017) 98–105, https://doi.org/10.22219/jemmme.v2i2.5053.
[35] K. Zhang, Y. Gu, M. li, Z. Zhang, Effect of rapid curing process on the properties of carbon fiber/epoxy composite fabricated using vacuum assisted resin infusion molding, Mater. Des. 54 (2014) 624–631, https://doi.org/10.1016/j.matdes.2013.08.065.
[36] Z. Liu, Y. Xia, S. Guo, Characterization methods of delamination in a plain woven CFRP composite, J. Mater. Sci. 54 (20) (2019) 13157–13174, https://doi.org/10.1007/s10853-019-03847-4.
[37] B. Wahyu, W. Artha, F. Rozaq, N. Faisal, 'Effect of fiber length on tensile strength , impact toughness , and flexural strength of Banana Stem Fiber, BSF 8 (1) (2023) 7–14, https://doi.org/10.22219/jemmme.v8i1.25570.
[38] P.J. Wibawa, M. Nur, M. Asy'ari, H. Nur, SEM, XRD and FTIR analyses of both ultrasonic and heat generated activated carbon black microstructures, Heliyon 6 (3) (2020), https://doi.org/10.1016/j.heliyon.2020.e03546.
[39] Y. Quan, Q. Liu, S. Zhang, S. Zhang, Comparison of the morphology, chemical composition and microstructure of cryptocrystalline graphite and carbon black, Appl. Surf. Sci. 445 (Jul. 2018) 335–341, https://doi.org/10.1016/J.APSUSC.2018.03.182.
[40] L. Vidya, Mandal, B. Verma, P.K. Patel, Review on polymer nanocomposite for ballistic & aerospace applications, Mater. Today Proc. 26 (xxxx) (2019) 3161–3166, https://doi.org/10.1016/j.matpr.2020.02.652.
[41] W.A. Wirawan, M.A. Choiron, E. Siswanto, T.D. Widodo, Morphology, structure, and mechanical properties of new natural cellulose fiber reinforcement from waru (Hibiscus tiliaceus) bark, J. Nat. Fibers (2022), https://doi.org/10.1080/15440478.2022.2060402.
[42] N. Reddy, Y. Yang, Properties of high-quality long natural cellulose fibers from rice straw, J. Agric. Food Chem. 54 (21) (2006) 8077–8081, https://doi.org/10.1021/jf0617723.
[43] K.A. Deshmukh, et al., Augmenting the wear performance of epoxy composites by different fillers: synthesis of highly crystalline g-C3N4 by simple pyrolysis and recycling of carbon fibres from old aircraft composites, Appl. Surf. Sci. Adv. 6 (2021) 100125, https://doi.org/10.1016/j.apsadv.2021.100125.
[44] Y. He, et al., Micro-crack behavior of carbon fiber reinforced Fe3O4/graphene oxide modified epoxy composites for cryogenic application, Compos. Part A Appl. Sci. Manuf. 108 (2018) 12–22, https://doi.org/10.1016/j.compositesa.2018.02.014. December 2017.
[45] A.F. Rigail-Cedeño, M. Espinoza-Andaluz, J. Vera, M. Orellana-Valarezo, M. Villacis-Balbuca, Influence of different carbon materials on electrical properties of epoxy-based composite for bipolar plate applications, Mater. Today Proc. 33 (xxxx) (2020) 2003–2007, https://doi.org/10.1016/j.matpr.2020.06.455.
[46] H. Mart, H. Yürük, M. Şaçak, V. Muradoğlu, A.R. Vilayetoğlu, The synthesis, characterization and thermal stability of oligo-4-hydroxybenzaldehyde, Polym. Degrad. Stab. 83 (3) (2004) 395–398, https://doi.org/10.1016/j.polymdegradstab.2003.08.003.
[47] N.D. Kambli, K.K. Samanta, S. Basak, S.K. Chattopadhyay, P.G. Patil, R. R. Deshmukh, Characterization of the corn husk fibre and improvement in its thermal stability by banana pseudostem sap, Cellulose 25 (9) (Sep. 2018) 5241–5257, https://doi.org/10.1007/S10570-018-1931-Z/METRICS.
[48] M.S. Asawthnarayan, B.M. Rudresh, M. Muniraju, H.N. Reddappa, Effect of abrasive frication on the wear behaviour glass –Epoxy Composites: effect of nanographene, Mater. Today Proc. 54 (xxxx) (2022) 209–216, https://doi.org/10.1016/j.matpr.2021.08.294.
[49] M. Alajmi, K.R. Alrashdan, T. Alsaeed, A. Shalwan, Tribological characteristics of graphite epoxy composites using adhesive wear experiments, J. Mater. Res. Technol. 9 (6) (2020) 13671–13681, https://doi.org/10.1016/j.jmrt.2020.09.106.
[50] Y. Bu, et al., Fabrication of low friction and wear carbon/epoxy nanocomposites using the confinement and self-lubricating function of carbon nanocage fillers, Appl. Surf. Sci. 538 (2021) 1–6, https://doi.org/10.1016/j.apsusc.2020.148109. October 2020.
[51] B. Suresha, N.M. Indushekhara, C.A. Varun, D. Sachin, K. Pranao, Effect of carbon nanotubes reinforcement on mechanical properties of aramid/epoxy hybrid composites, Mater. Today Proc. 43 (xxxx) (2020) 1478–1484, https://doi.org/10.1016/j.matpr.2020.09.307.
[52] Z. Salleh, M.M. Islam, M.Y.M. Yusop, M.A.M.M. Idrus, Mechanical properties of activated carbon (AC) coconut shell reinforced polypropylene composites encapsulated with epoxy resin, APCBEE Proced. 9 (2014) 92–96, https://doi.org/10.1016/j.apcbee.2014.01.017. Icbee 2013.
[53] N.H. Sari, S. Suteja, M.N. Samudra, H. Sutanto, Composite of Hibiscus tiliaceus stem fiber/polyester modified with carbon powder : synthesis and characterization of tensile strength , flexural strength and morphology properties in press , accepted manuscript – note to user, Int. Nanoelectron. Mater. 14 (3) (2021) 1–13.
[54] P. Kurniasih, et al., Flammability and morphology of Agel leaf fibre- epoxy composite modified with carbon powder for fishing boat applications, Arch. Mater. Sci. Eng. 122 (1) (2023) 13–21, https://doi.org/10.5604/01.3001.0053.8842.
[55] K. Olszowska, et al., Development of epoxy composites with graphene nanoplatelets and micro-sized carbon foam: morphology and thermal, mechanical and tribological properties, Tribol. Int. 185 (April) (2023), https://doi.org/10.1016/j.triboint.2023.108556, 0–2.
[56] U. Szeluga, et al., Effect of grain fractions of crushed carbon foam on morphology and thermomechanical and tribological properties of random epoxy-carbon composites, Wear 466–467 (2021), https://doi.org/10.1016/j.wear.2020.203558. November 2020.
[57] S. Bal, Experimental study of mechanical and electrical properties of carbon nanofiber/epoxy composites, Mater. Des. 31 (5) (2010) 2406–2413, https://doi.org/10.1016/j.matdes.2009.11.058.
[58] N.H. Sari, et al., Morphology and mechanical properties of coconut shell powder-filled untreated cornhusk fibre-unsaturated polyester composites, Polymer (Guildf) 222 (March) (2021) 123657, https://doi.org/10.1016/j.polymer.2021.123657.
[59] L. Yue, G. Pircheraghi, S.A. Monemian, I. Manas-Zloczower, Epoxy composites with carbon nanotubes and graphene nanoplatelets - dispersion and synergy effects, Carbon N. Y. 78 (2014) 268–278, https://doi.org/10.1016/j.carbon.2014.07.003.
[60] Y.C. Chiou, H.Y. Chou, M.Y. Shen, Effects of adding graphene nanoplatelets and nanocarbon aerogels to epoxy resins and their carbon fiber composites, Mater. Des. 178 (2019), https://doi.org/10.1016/j.matdes.2019.107869.
[61] H.P.S. Abdul Khalil, P. Firoozian, I.O. Bakare, H.M. Akil, A.M. Noor, Exploring biomass based carbon black as filler in epoxy composites: flexural and thermal properties, Mater. Des. 31 (7) (2010) 3419–3425, https://doi.org/10.1016/j.matdes.2010.01.044.
[62] N.K. Chandramohan, Variation in compressive and flexural strength of the carbon epoxy composites with the addition of various fillers to the epoxy resin, Mater. Today Proc. 21 (xxxx) (2020) 643–647, https://doi.org/10.1016/j.matpr.2019.06.731.